

## Achievement of Reactor-Relevant $\beta$ in Low- $q$ Divertor Discharges in the Doublet III-D Tokamak

T. S. Taylor, E. J. Strait, L. Lao, A. G. Kellman, T. H. Osborne, K. Burrell, M. S. Chu, J. C. DeBoo, H. Fukumoto,<sup>(a)</sup> P. Gohil, R. Groebner, C. Hsieh, G. Jackson, S. Kinoshita,<sup>(a)</sup> P. Lomas,<sup>(b)</sup> R. Snider, H. St. John, R. D. Stambaugh, R. E. Stockdale, and A. D. Turnbull

*General Atomics, San Diego, California 92138*

(Received 15 April 1988)

A volume-average toroidal  $\beta$  of 6.2% has been obtained with 10 MW of hydrogen-neutral-beam injection into deuterium divertor discharges in DIII-D. High- $\beta$  discharges were maintained quiescently for many energy confinement times in elongated,  $\kappa=2$ , divertor discharges where the safety factor at the 95% flux surface was near 2. The maximum  $\beta$  calculated to be stable against ideal kinks and ideal ballooning modes is 8.5%–9.5%, confirming that these  $I/aB \approx 2.5$  MA/mT discharges are some distance below the stability limit.

PACS numbers: 52.55.Fa, 52.35.-g, 52.50.Gj

Because of economic and engineering considerations, an ignited tokamak fusion reactor must operate reliably with the ratio of the plasma pressure to the toroidal magnetic field pressure (volume-average toroidal beta,  $\beta_T$ ) in excess of 4%.<sup>1</sup> Scaling of the maximum stable  $\beta$ ,<sup>2-5</sup> and the energy confinement time,<sup>6,7</sup> dictates that a tokamak fusion reactor must operate at low values of the safety factor  $q$  and high plasma current (the safety factor is a measure of the helical pitch of the magnetic field lines). Furthermore, operation at high  $\beta_T$  and low  $q$  is best demonstrated in a magnetic configuration with a poloidal magnetic divertor, because of the high-confinement regime of operation ( $H$  mode) found in present divertor tokamaks.<sup>8,9</sup>

In this Letter we report the first achievement in a large tokamak of a volume-average  $\beta$  in excess of 6% in an elongated low- $q$  divertor discharge, an increase by more than a factor of 2 over  $\beta$  values previously reported in divertor discharges. All of the gross parameters of these high- $\beta$  discharges, including plasma current, stored energy, discharge shape, line-average density, and internal inductance, were varying at most very slowly for many energy replacement times. The duration of the high- $\beta$  phase of these discharges was limited by the duration of the high-power neutral injection, and  $\beta_T$  has been maintained above 5% for nearly 1 s.

The maximum achievable  $\beta$  is limited by both stability and power balance. Theoretically predicted  $\beta$  limits due to ideal ballooning and ideal external kinks are approximated by<sup>10-13</sup>

$$\beta_T(\text{stability}) \leq C_\beta \frac{I}{aB} \cong C_\beta \frac{2\pi}{\mu_0} \frac{\epsilon}{q_{\text{cyl}}} \frac{1+\kappa^2}{2}. \quad (1)$$

Here  $I/aB = I_N$  is the normalized current,  $I$  is the total plasma current,  $a$  is the plasma minor radius,  $B$  is the vacuum toroidal field,  $\epsilon = a/R$  is the inverse aspect ratio, with  $R$  the major radius of the discharge,  $\kappa$  is the vertical elongation of the plasma cross section, and  $q_{\text{cyl}}$  is the

cylindrical approximation to the safety factor. The coefficient  $C_\beta$  depends on the instability responsible for the limit and the choice of the pressure and current profiles. The value of  $C_\beta$  determined from several experiments is  $2.8 \leq C_\beta \leq 3.6$  %/(MA/mT).<sup>2-5</sup> The maximum  $\beta$  is also limited by power balance to

$$\beta_T(\text{energetics}) = \frac{4\mu_0}{3} \frac{a}{V} \frac{P_{\text{tot}}}{B} \frac{\tau_E}{I} I_N, \quad (2)$$

where  $\tau_E$  is the global energy confinement time,  $P_{\text{tot}}$  is the total input power, and  $V$  denotes volume. The  $\tau_E$  of beam-heated discharges is proportional to plasma current,<sup>8,9</sup> so that  $\tau_E/I$ , the confinement quality, is roughly constant, independent of plasma current. High- $\beta$  operation, from both stability and power-balance considerations, requires high normalized current or, equivalently, low  $q$ . Because the confinement quality of  $H$ -mode divertor discharges is roughly twice that of  $L$ -mode discharges,<sup>8,9</sup> the high- $\beta$  experiments in DIII-D have been carried out in divertor discharges, where the  $H$  mode is obtained.

Stable operation of divertor discharges at  $q \approx 2$  has allowed the range of normalized current for which high- $\beta$  experiments can be reliably carried out to be increased to 2.5 MA/mT in DIII-D, more than a factor of 2 improvement over that obtained in Doublet-III divertor discharges, where  $I_N$  was limited to 1.1 MA/mT (see Fig. 1). Elongated,  $\kappa \approx 2$ , near-steady-state divertor discharges have been stably operated with a safety factor at the 95% flux surface of  $q_{95} = q((\psi - \psi_0)/(\psi_a - \psi_0)) = 0.95 = 2.0$ , in both Ohmically heated and beam-heated discharges. These low- $q$  discharges can be operated reproducibly and terminated quiescently and without disruption. In divertor discharges with a plasma current ramp,  $q_{95} = 1.8$  has been reached transiently. Similar results have been obtained in limiter discharges where  $q_{95} = 2.1$  has been obtained in steady state and  $q_{95} = 2.0$  has been obtained transiently. Although there

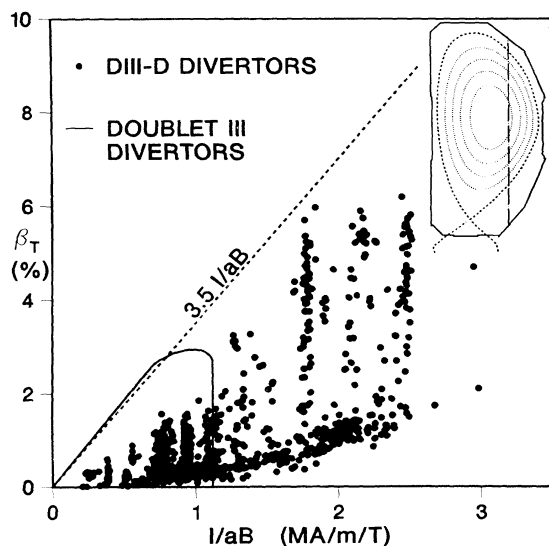


FIG. 1. Operating regime of DIII-D divertor discharges. The dashed line represents the scaling of maximum achievable  $\beta$  from Doublet III (Ref. 3). The solid line shows the envelope of Doublet-III divertor discharges. Inset: Equilibrium flux surfaces of the highest- $\beta$  discharge (55390).

has not been an extensive effort to establish a  $q$  limit in DIII-D, we believe that  $q_{95} = 2.0 \pm 0.2$  represents the minimum in both DIII-D elongated limiter and divertor discharges.

A volume-average toroidal  $\beta$  of greater than 5% has been repeatedly obtained and maintained quiescently for many energy confinement times in these low- $q$  divertor discharges, and  $\beta$  near 6% has been reached in several discharges.  $\beta_T = 2\mu_0 \langle p \rangle / B^2$ , where  $\langle p \rangle$  is the volume-average plasma pressure and  $B$  is the toroidal field taken at the center of the last closed-flux surface. These are deuterium discharges with up to 10 MW of neutral (hydrogen) beam heating from seven ion sources. To demonstrate that high  $\beta$  can be obtained in steady state, the temporal evolution of a discharge with  $\beta_T = 5.6\%$  is shown in Fig. 2. The auxiliary heating begins at  $t = 1.6$  s after a nearly steady-state ohmic discharge is established. The beam heating is increased to 6 MW at 1.82 s and the discharge makes a transition into  $H$  mode<sup>8,9</sup> 10 ms later as evidenced by the sudden drop in the divertor  $D_\alpha$  and the abrupt rise in the line-average density and  $\beta_T$ .  $\beta$  continues to rise as the beam heating is increased, reaching a maximum value at 2.6 s. The only prominent MHD activity in this discharge is the usual  $n=1$  internal-kink activity associated with the sawteeth on the soft-x-ray emission, and the edge-localized modes<sup>14</sup> seen as large short bursts on the divertor  $D_\alpha$  emission. This temporal evolution differs from that in previous tokamak experiments with  $\beta > 4\%$  where the high values of  $\beta_T$  were obtained with the use of current ramps during high-power injection to obtain stable profiles.<sup>15,16</sup>

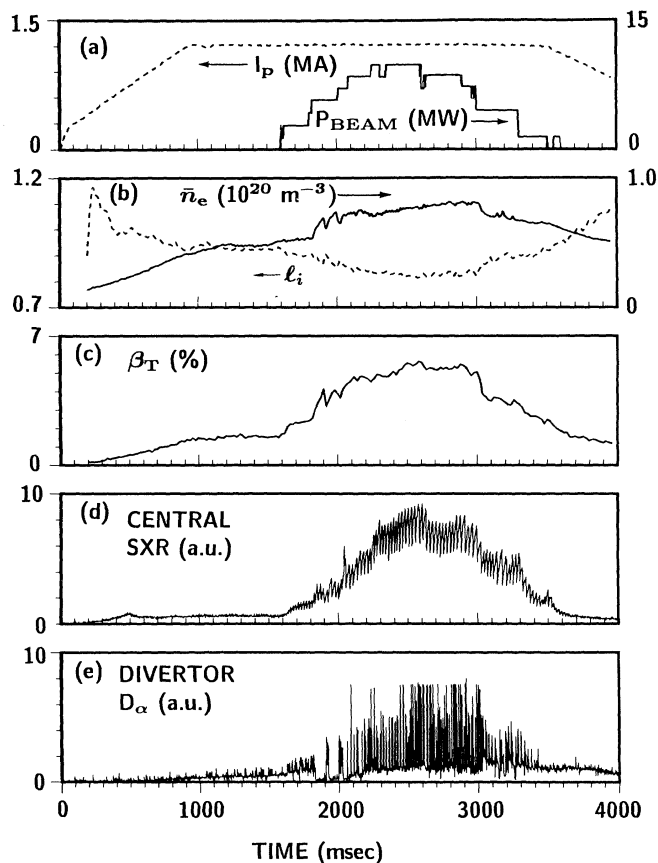


FIG. 2. Temporal evolution of a typical high- $\beta$  discharge. (a) Plasma current and neutral-beam-heating power; (b) line-average electron density ( $\bar{n}_e$ ), and plasma internal inductance ( $l_i$ ); (c) volume-average toroidal  $\beta$ ; (d) soft-x-ray emission from a central chord; (e)  $D_\alpha$  emission from the divertor region.  $\beta_T$  and  $l_i$  are determined from the MHD equilibrium analysis.

The highest  $\beta$  achieved to date in DIII-D is  $\beta_T = 6.2\%$  in a low- $q$  elongated divertor discharge. An equilibrium flux plot of this high- $\beta$  discharge is shown as an inset of Fig. 1, and the results of analyses are listed in Table I.  $\beta$  can be determined from an equilibrium fit using only the poloidal magnetic measurements (poloidal flux loops, internal magnetic probes, and a plasma current Rogowski), yielding  $(\beta_{T\parallel} + \beta_{T\perp})/2 = 5.9\%$ . The diamagnetic flux gives a value of  $\beta_{T\perp} = 6.2\%$ .

From a more complete calculation of  $\beta$  using kinetic data,  $\beta_T^{\text{kin}} = (\beta_{T\parallel} + 2\beta_{T\perp})/3 = 6.2\%$  is obtained in good agreement with equilibrium and diamagnetic values. The electron temperature and density profiles are measured with a multipoint Thomson scattering system along the vertical chord as shown in the inset of Fig. 1. The line-integrated density is measured by a laser interferometer along a vertical chord at the same radius as the Thomson scattering, and the electron density measured by the Thomson scattering is normalized to the

TABLE I. Summary of the highest- $\beta$  discharge (55390).

|   |                                  |
|---|----------------------------------|
| $\beta_T$                               | $6.2 \pm 0.5\%$                  |
| $(\beta_{\perp} + \beta_{\parallel})/2$ | 5.9%                             |
| $\beta_{\perp}$                         | 6.2%                             |
| $\beta_{\text{kin}}$                    | $6.2\% \pm 0.9\%$                |
| $\beta_{\text{electrons}}$              | 3.0%                             |
| $\beta_{\text{thermal ions}}$           | 2.8%                             |
| $\beta_{\text{fast ions}}$              | 0.4%                             |
| $I_N$                                   | 2.5 MA/Tm                        |
| $\beta_T/I_N$                           | 2.5% Tm/MA                       |
| $I_p$                                   | 1.2 MA                           |
| $B$                                     | 0.8 T                            |
| $a$                                     | 0.616 m                          |
| $\kappa$                                | 1.95                             |
| $q_{95}$                                | 2.1                              |
| $V$                                     | 21.9 m <sup>3</sup>              |
| $P_{\text{tot}}$                        | 10.4 MW                          |
| $P_{\text{beam}}$                       | 9.8 MW ( $H^0 \rightarrow D^+$ ) |
| $\tau_E$                                | 51 ms                            |
| $\bar{n}_e$                             | $0.83 \times 10^{20}/\text{m}^3$ |
| $T_e(0)$                                | 1 keV                            |
| $T_i(0)$                                | 1 keV                            |
| $Z_{\text{eff}}$                        | 1.3                              |

measured line-integral density. The ion temperature profile is measured with a multichord charge-exchange recombination system. Visible bremsstrahlung measurements are made along sixteen tangential chords to obtain  $Z_{\text{eff}}$ . The temperatures, density, and  $Z_{\text{eff}}$  are assumed constant on a flux surface and the discharge shape from the MHD equilibrium is combined with the geometry of the diagnostics in the ENERGY<sup>17</sup> code to give the relevant quantities in terms of an equivalent radial coordinate. The measured data were fitted with a cubic spline and the smoothed profiles were then used as input to the ONETWO<sup>18</sup> transport code, to calculate the fast-ion pressure. The neutral-beam deposition profile was calculated with the NFREYA<sup>19</sup> code. The total pressure is shown in Fig. 3(a).

This discharge with  $\beta_T = 6.2\%$  is calculated to be stable against ideal kink modes and ideal ballooning modes. The stability of internal kinks,  $n = 1-3$  and ballooning modes depends on the details of the current density profile and the pressure profile. To obtain self-consistent current density and pressure profiles, the total pressure profile from the transport code is used as input to the MHD equilibrium analysis.<sup>20</sup> In addition, the  $q = 1$  surface is taken to be at the sawtooth inversion radius. These additional inputs further constrain the allowed current profiles. The pressure profile from this equilibrium analysis differs only slightly from the profile from the transport code as seen in Fig. 3(a).

Stability against ideal kinks was calculated using the GATO<sup>21</sup> code and the analysis shows this 6.2% discharge to be stable to  $n = 1$ ,  $n = 2$ , and  $n = 3$  kinks with no wall stabilization. Kink analysis of theoretical equilibria with

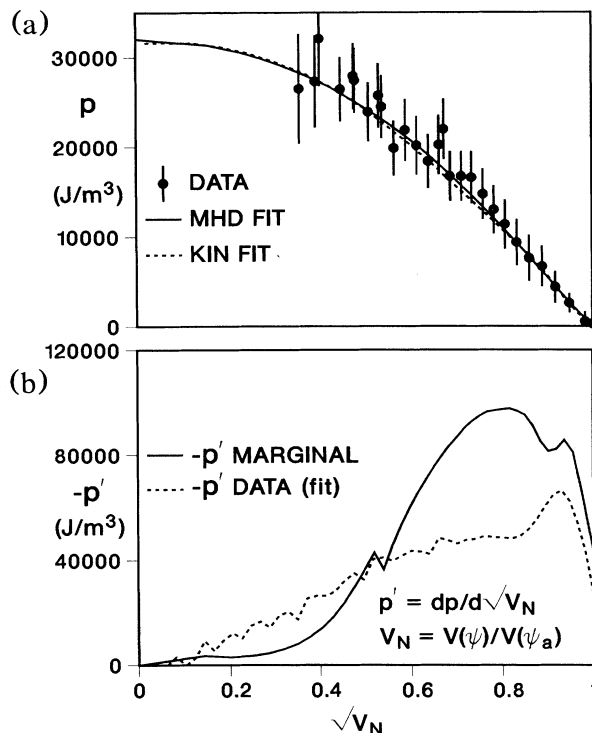


FIG. 3. (a) Pressure profiles of the highest- $\beta$  discharge (55390) at 2.7 s. The data points are the sum of the electron and thermal-ion pressures and the calculated fast-ion pressure. The dashed curve is the calculated total pressure from the transport code ONETWO. The solid curve is the self-consistent calculation from the equilibrium code EFIT. The abscissa,  $\sqrt{V_N}$ , is an equivalent radial coordinate. (b) The pressure gradient profiles. The solid curve is the marginal gradient calculated with the code MBC. The dashed curve is the measured gradient from the kinetic analysis, calculated from ONETWO.

the same shape and similar current profiles as those for the highest- $\beta$  discharge, but with higher pressure, indicates that the maximum  $\beta$  stable against  $n = 1$  ideal kinks with no wall stabilization is 8.5%.

A  $\beta$  value of 6.2% in the  $I_N = 2.5$  discharge is substantially below that consistent with marginal stability to ballooning modes. The pressure gradient that is marginally stable against ideal ballooning modes is calculated using the procedure outlined by Greene and Chance<sup>22</sup> using the ballooning code MBC.<sup>23</sup> The marginal gradient is compared to the gradient from the measured profile in Fig. 3(b). The local pressure gradient is significantly below that marginally stable to ballooning modes in the outer region of the discharge. The pressure gradient in the center of the discharge is calculated to be near or above the marginally stable gradient, although the uncertainty in both the pressure profile and the current density profile is large near the axis. The  $\beta$  that is consistent with the marginal curve shown in Fig. 3(b), i.e., marginally stable to ideal ballooning modes at every sur-

face, is 9.4%.

Our highest  $\beta$  discharges at  $I_N = 2.5$  MA/mT are well below limits extrapolated from experimental data and theoretical predictions. The maximum stable  $\beta$  extrapolated from Doublet-III data is 8.8%, which is in rough agreement with the  $n=1$  kink and ballooning calculations.  $\beta$  near 6% has been obtained at several values of normalized current,  $1.8 < I_N < 2.5$  MA/mT, or equivalently  $3.2 > q_{95} > 2.1$ , as shown in Fig. 1. In general, the highest- $\beta$  discharges in Fig. 1 do not represent stability limits, but rather limitations of available heating power and energy confinement time. A possible exception is the group of discharges at maximum normalized  $\beta$ ,  $\beta_N = \beta_T / I_N$ , where  $\beta$ -related instabilities are observed, causing  $\beta$  saturation or  $\beta$  collapse in some cases.<sup>24</sup> In contrast, the envelope of Doublet-III data shown in Fig. 1 does represent limits of stability.

The achievement of 6.2%  $\beta$  in divertor  $H$ -mode plasmas in DIII-D at high elongation and low  $q$  represents a significant advance in stable high- $\beta$  operation in divertor discharges (2.9% in Doublet III) and qualifies the divertor  $H$ -mode operation scenario for tokamaks as a viable candidate for high- $\beta$  ignited tokamak reactors. The stable operation for many confinement times under near stationary conditions indicates that tokamaks may indeed operate in steady state at high  $\beta$ .

The authors would like to thank Dr. J. Ferron for helpful discussions in preparing the manuscript, and W. Howl for assistance with the computations. The experimental results reported here were made possible only by the diligent support of the entire DIII-D Physics Group, the Tokamak Operations Group, the Neutral Beam Group, the Engineering Group, and collaborators from other laboratories. This work was sponsored by the Department of Energy under Contract No. DE-AC03-84ER51044.

<sup>(a)</sup>On assignment from Hitachi Ltd., Hitachi-shi, Ibaraki, 316 Japan.

<sup>(b)</sup>On assignment from JET Joint Undertaking, Abingdon, Oxfordshire, England.

<sup>1</sup>J. Sheffield, Nucl. Fusion **25**, 1733 (1985).

<sup>2</sup>R. D. Stambaugh *et al.*, in *Proceedings of the Tenth International Conference on Plasma Physics and Controlled Nuclear Fusion, London, 1984* (International Atomic Energy Agency, Vienna 1985), Vol. 1, p. 217.

<sup>3</sup>K. Bol, M. Okabayashi, and R. Fonck, Nucl. Fusion **25**, 1149 (1985).

<sup>4</sup>G. H. Neilson *et al.*, Nucl. Fusion **25**, 825 (1985).

<sup>5</sup>M. Keilhacker and ASDEX Team, Nucl. Fusion **25**, 1045 (1985).

<sup>6</sup>S. M. Kaye and R. J. Goldston, Nucl. Fusion **25**, 65 (1985).

<sup>7</sup>J. C. DeBoo *et al.*, Nucl. Fusion **26**, 211 (1986).

<sup>8</sup>F. Wagner *et al.*, Phys. Rev. Lett. **49**, 1408 (1982).

<sup>9</sup>K. H. Burrell *et al.*, Phys. Rev. Lett. **59**, 1432 (1987).

<sup>10</sup>L. C. Bernard, F. J. Helton, R. W. Moore, and T. N. Todd, Nucl. Fusion **23**, 1475 (1983).

<sup>11</sup>F. Troyon, T. Gruber, H. Sauremann, S. Semzato, and S. Succi, in *Proceedings of the Eleventh European Conference on Plasma Physics and Controlled Fusion Aachen, 1983* (European Physical Society, Petit-Lancy, 1983), Vol. 26, No. 1A, p. 209.

<sup>12</sup>J. A. Wesson and A. Sykes, Nucl. Fusion **25**, 85 (1985).

<sup>13</sup>K. Yamazaki *et al.*, Nucl. Fusion **25**, 1543 (1985).

<sup>14</sup>M. Keilhacker *et al.*, Plasma Phys. **26**, 1453 (1984).

<sup>15</sup>K. H. Burrell *et al.*, Nucl. Fusion **23**, 536 (1983).

<sup>16</sup>K. Bol *et al.*, Phys. Rev. Lett. **57**, 1891 (1986).

<sup>17</sup>H. St. John, G. L. Jahns, K. H. Burrell, and J. C. DeBoo, Bull. Am. Phys. Soc. **32**, 1897 (1987).

<sup>18</sup>W. W. Pfeiffer, R. H. Davidson, R. L. Miller, and R. E. Waltz, General Atomics Report No. GA-A16178, 1980 (unpublished).

<sup>19</sup>G. G. Lister, D. E. Post, and R. Goldston, in *Proceedings of the Third Symposium on Plasma Heating in Toroidal Devices, Varenna, 1974* (Editrice Compositori, Bologna, 1976) p. 303.

<sup>20</sup>L. Lao, H. St. John, R. J. Groebner, W. Howl, and T. S. Taylor, in *Proceedings of the Twelfth Conference on the Numerical Simulation of Plasmas, San Francisco, September 1987* (to be published).

<sup>21</sup>L. C. Bernard, F. J. Helton, and R. W. Moore, Comput. Phys. Commun. **24**, 377 (1981).

<sup>22</sup>J. M. Greene and M. S. Chance, Nucl. Fusion **21**, 453 (1981).

<sup>23</sup>R. W. Moore, General Atomics Report No. GA-A17243 1981 (unpublished).

<sup>24</sup>E. J. Strait *et al.*, following Letter, Phys. Rev. Lett. **62**, 1282 (1989).